Т. 8. №6. 2022
https://doi.org/10.33619/2414-2948/79

UDC 681.7.064.454 https://doi.org/10.33619/2414-2948/79/48

DESIGN AND ANALYSIS OF ANTIREFLECTION LAYER ON THE SURFACE OF CRYSTALLINE SILICON SOLAR CELL

*©**Yilie Zhao**, ORCID: 0000-0003-0034-6338, Ogarev Mordovia State University, Saransk, Russia, 736052714@qq.com*

ДИЗАЙН И АНАЛИЗ ПРОСВЕТЛЯЮЩЕГО ПОКРЫТИЯ НА ПОВЕРХНОСТИ КРИСТАЛЛИЧЕСКОГО КРЕМНИЯ СОЛНЕЧНОГО ЭЛЕМЕНТА

*©**Вилли Чжао,** ORCID: 0000-0003-0034-6338, Национальный исследовательский Мордовский государственный университет имени Н. П. Огарёва, г. Саранск, Россия, 2213831907@qq.com*

Abstract. With the positive development of photovoltaic technology, improving efficiency and reducing cost has become a global problem facing the solar industry. The development of solar cell anti-reflection film can significantly reduce the reflection of sunlight on the surface of the battery, increase the flux of light entering the battery, and create more photo-generated carriers, which is the most economical and effective way to improve the efficiency of the battery. More photo-generated carriers are produced, which is the most economical and effective way to improve the efficiency of batteries. Therefore, it's of great value to explore a performance-matched antireflective film material for solar cells and its preparation process. The plasma enhanced chemical vapor deposition of silicon nitride antireflective coatings has been widely used in photovoltaic industry. The aim is to form an antireflection film on the surface of crystalline silicon solar cells and achieve good passivation effect. The thickness and refractive index of the antireflective film have an important influence on the performance of the battery. It is of great significance to explore the optimum technological conditions for preparing the optimum thin films. Considering the optical properties, stability, preparation process and production cost of antireflective film materials, the influence of antireflective film on the output characteristics of solar cells was studied by using PC1D simulation software.

Аннотация. С положительным развитием фотоэлектрических технологий повышение эффективности и снижение затрат стало глобальной проблемой, стоящей перед солнечной промышленностью. Разработка антибликовой пленки для солнечных батарей может значительно уменьшить отражение солнечного света на поверхности батареи, увеличить поток света, попадающего в батарею, и создать больше фотогенерируемых носителей, что является наиболее экономичным и эффективным способом улучшения эффективность аккумулятора. Выпускается больше фотогенерируемых носителей, что является наиболее экономичным и эффективным способом повышения эффективности батарей. Поэтому очень важно изучить антибликовый пленочный материал с соответствующими характеристиками для солнечных элементов и процесс его изготовления. Плазменное химическое осаждение из паровой фазы антиотражающих покрытий из нитрида кремния широко используется в фотоэлектрической промышленности. Цель состоит в том, чтобы сформировать просветляющую пленку на поверхности солнечных элементов из кристаллического кремния и добиться хорошего пассивирующего эффекта. Толщина и показатель преломления антиотражающей пленки оказывают большое влияние на характеристики батареи. Большое

Т. 8. №6. 2022
https://doi.org/10.33619/2414-2948/79

значение имеет исследование оптимальных технологических условий получения оптимальных тонких пленок. Принимая во внимание оптические свойства, стабильность, процесс подготовки и стоимость производства просветляющих пленочных материалов, влияние просветляющей пленки на выходные характеристики солнечных элементов было изучено с использованием программного обеспечения для моделирования PC1D.

Keywords: Solar energy battery，Decreased membrane，Reflaectivity curve，PC1D.

Ключевые слова: батарея солнечной энергии, Уменьшает мембрану, Кривая отражательной способности, PC1D.

1. Introduction

Social development and human progress are closely related to energy. Now more than 80% of the energy used by mankind is obtained by burning fossil fuels such as coal, oil and natural gas, which will emit a large amount of harmful gases and dust such as carbon dioxide, sulfur dioxide and nitric oxide, resulting in environmental pollution and global warming [1]. Moreover, the reserves of primary energy will also be exhausted. The top priority is to develop green and safe renewable energy. As we all know, sunshine is inexhaustible, non regional and pollution-free. It can be said that it has become the first choice of new energy. It is estimated that the energy obtained by the earth from the sun per unit time is ten million times faster than the global energy consumption; The average amount of radiation received by the earth's surface per square meter per year can produce nearly 2000 degrees of electricity. According to the data of the International Energy Agency, 6% of the global demand for solar panels can be fully met if they are installed in desert areas [2]. So it seems that the development of solar photovoltaic industry is of great significance.

With the lack of global energy, the consumption of primary energy is increasing, and the problem of pollution has become urgent. Solar energy is widely distributed and is the center of global energy development [3, 4]. According to scientific estimates, by 2050, renewable energy will account for more than 30% of total energy consumption. In 50 years, renewable energy will account for 80% of the world energy organization.

What's more worth mentioning is that aside from the problem of insufficient fossil energy storage, the environmental problems caused by the combustion of fossil energy are also a hot topic today. The combustion of fossil energy will emit a large amount of sulfide and carbon dioxide gases. The former mainly forms acid rain, endangers farmers, trees and destroys buildings, while the latter is a greenhouse gas, which will reduce the temperature and reflect the atmosphere from the earth's surface, leading to global climate warming and glacier melting, Then the sea level rises, and some low-altitude cities and even countries will be inundated. In addition, global warming will make severe weather such as drought and flood occur frequently, which poses a serious threat to human life and property purchase. Moreover, burning fossil energy will produce harmful particles and increase PM2 The concentration of 5 seriously affects human health.

Table 1-1

CURRENT SITUATION OF RENEWABLE ENERGY UTILIZATION IN 2020

Energy category	*Total resources (GW)*	*Theoretical development(GW)*	*Development degree(%)*	*Current installed capacity（GW）*
Small hydropower	125	115	65	50
Wind power generation	10000	1000	10	44
Biomass energy	300	100	30	33
Solar energy	9600000	109000	1	3613

Т. 8. №6. 2022
https://doi.org/10.33619/2414-2948/79

As mentioned above, there are countless problems caused by fossil fuels. The urgent task is to find renewable clean energy to replace fossil fuels, which plays a great role in human sustainable development in the future [5]. Nowadays, renewable energy includes hydropower, wind energy, solar energy, biomass energy, etc. Among them, biomass energy is related to food production and ecological environment, and it is unlikely to make large use of the most important energy. As shown in table 1-1, solar energy is the largest in terms of total resources. The energy of one hour of solar irradiation is equal to the energy required by human beings on earth in a year. Its theoretical exploitable value is also the highest, but its degree of development is only 1%. It can be seen that researchers still have many problems to be solved in the development and utilization of solar energy [6].

In addition, solar energy is very common. There is no need to explore every corner of the earth. Transportation can be developed and utilized directly. It is one of the most primitive development and utilization of pollution-free energy. In the era when the environment is deteriorating and the energy problem is paid more and more attention, this is a very obvious advantage.

2. Basic theory of solar cell

2.1 structure and power generation principle of crystalline silicon solar cell

In fact, solar cells are semiconductor devices that convert light energy into electrical energy. If you want to know more about the principle and structure of the battery, you must first understand it. In this way, we can sum up the reasons for the low conversion rate of solar cells, and the cost and conversion rate are the factors restricting the further development of solar cells.

2.1.1 structure of crystalline silicon solar cell

At present, crystalline silicon solar cells are mainly non monocrystalline silicon solar cells and polycrystalline silicon solar cells. Monocrystalline silicon cells have high cost because of their high purity of silicon materials. However, it has mature manufacturing technology, high stability, weak photoinduced decay and higher conversion efficiency than polycrystalline silicon cells [7, 8].

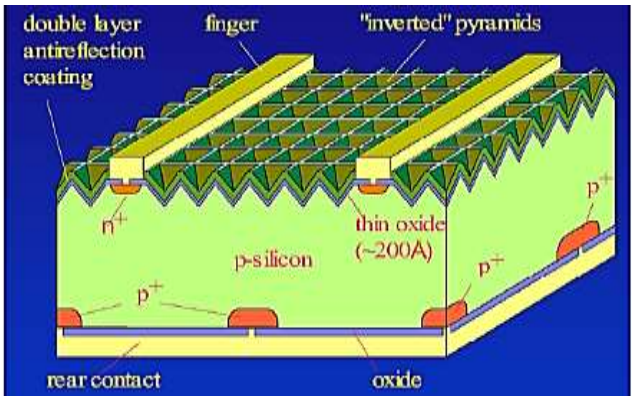

Figure 1. Structure of Perl battery

The conversion efficiency of Perl (passivated emitter, reverse point dispersion) solar cell developed by Zhao Jianhua, deputy director of silicon solar cell and Silicon Luminescence laboratory at the University of New South Wales, Australia, is as high as 24.7% [9]. So far, it has maintained the highest record of conversion efficiency. As shown in Figure 1, the upper and lower surfaces are passivated by oxide film to reduce the rapid recombination of minority carriers. In order to reduce the reflection of light and increase absorption, two layers of antireflection films are

Т. 8. №6. 2022
https://doi.org/10.33619/2414-2948/79

also plated on the surface of crystalline silicon cells. In addition, a light trapping structure is prepared to increase the distance of light in crystalline silicon and promote photons to excite more carriers.

In reproduction and manufacturing, p-type silicon material is mostly used as the substrate. The n-type silicon material prepared on the surface of the substrate is the most emitter, and the phosphorus diffusion process is adopted. P-N structure is formed, and the reflectivity of solar cells is reduced by depositing silicon nitride film and flocking surface structure [10].

Brush a layer of aluminum on the back of the battery, so that the back of the battery can be emitted back to the battery, forming the re absorption of photons and exciting more carriers. Collect current and print electrodes on the top and bottom.

2.2 optical design

2.2.1 antireflection film

Figure 2-2 illustrates the principle of quarter wavelength antireflection film. When the light reflected by the second interface returns to the first interface, the phase difference between the light reflected by the first interface and the light reflected by the first interface is 180°, so the former offsets the latter to a certain extent [11].

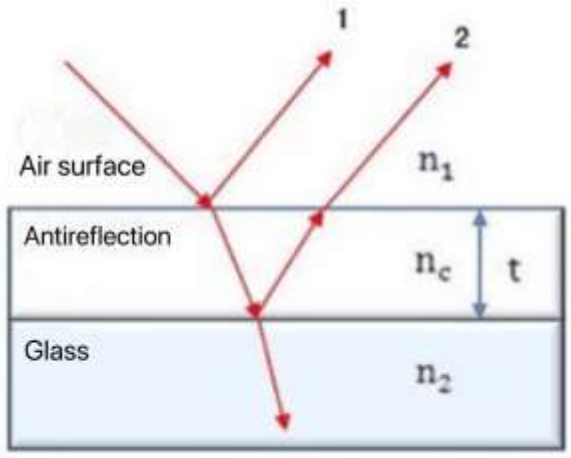

Figure 2-2. Dry light produced by quarter wavelength antireflection film

If the refractive index of the antireflection film is the geometric average of the refractive indexes of the materials on both sides ($n_1^2 = n_0 \cdot n_2$), (the reflectivity is for λ0) For silicon cells in air (nsi≈3.8), the best refractive index of antireflection film is the square root of silicon refractive index (i.e.nm≈1.9) [12]. When the silicon surface is covered with the best refractive index antireflection film, the relationship between the percentage of incident light reflected from the silicon surface and the wavelength. The antireflection film is designed to produce minimum reflection at a wavelength of 600nm. The weighted average value of the proportion of available sunlight reflected by the silicon surface coated with antireflection film can be maintained at about 10%.On the contrary, the reflectivity of bare silicon surface to available sunlight may exceed 30%. Batteries are usually encapsulated under glass or embedded in materials with refractive index (n≈1.5) similar to glass. This increases the optimum value of the refractive index of the antireflection film to about 2.3. The reflection of light by the battery covered with antireflection film with refractive index of 2.3 is also obvious before and after packaging. The refractive index of some antireflection film materials used in commercial solar cells is listed in Table 2-1. In addition to having a suitable refractive index, the antireflection film material must also be transparent.

Т. 8. №6. 2022
https://doi.org/10.33619/2414-2948/79

Antireflection films are often deposited as amorphous or amorphous thin layers to prevent light scattering at grain boundaries. The antireflection layer formed by vacuum evaporation will generally produce absorption in the ultraviolet wavelength region. However, the antireflection film made by oxidation or anodization of the deposited metal thin layer or the antireflection film made by chemical deposition process often has a "glass" structure, which will reduce UV absorption.

Multilayers made of different antireflection materials can improve the performance. The design of this multilayer film is more complex, but it can reduce reflection in a wide band. At least one manufacturer used two layers of antireflection film on high-efficiency batteries, which reduced the reflectivity of available sunlight to 4%.

Table 2-1

REFRACTIVE INDEX OF MATERIALS USED FOR ANTIREFLECTION FILM

Material	*Refractive index*
MgF_2	1.3~1.4
SiO_2	1.4~1.5
Al_2O_3	1.8~1.9
SiO	1.8~1.9
TiO_2	~2.3
ZnS	2.3~2.4

2.2.2 Suede

This suede is made by a selective corrosion on the silicon surface. This corrosion method makes the corrosion of silicon lattice structure in one direction much faster than that in the other direction. This exposes some planes in the lattice. In those small pyramids that look like pyramids, they are formed by these intersecting crystal planes. According to Miller index, the silicon surface of suede battery is usually parallel to 100 faces, and the pyramid is formed by the intersection of 111 faces. Diluted sodium hydroxide (NaOH) solution is usually used as selective corrosive agent.

The angle of the pyramid is determined by the orientation of the crystal plane. These spires give incident light at least two chances to enter the battery. If 33% is reflected at each incident point as in the case of vertical irradiation on the bare silicon surface, the total reflection is 0.33×0.3, about 11%. If an antireflection film is used, the reflection of sunlight can be kept below 3%. Even without antireflection film, when embedded in a material with refractive index similar to glass, the reflection is only about 4%. Another desirable feature is the angle between the light emitted by a and the silicon surface, so that the light can be absorbed closer to the battery surface. This will increase the collection probability of the battery, especially for the long wave part with weak absorption.

Suede also has some disadvantages. First, be more careful in operation; Second, such a surface will more effectively absorb all wavelengths of light, including those photons that do not want to be absorbed. The energy is not enough to produce the infrared radiation of electron hole pairs, which often raises the temperature of the battery. In addition, the metal upper electrode must extend up and down along the side of the pyramid. If the thickness of the metal layer is less than or equal to the height of the pyramid (~10mm), in order to maintain the same ohmic loss as on the flat surface, two to three times the metal material must be used.

3 Simulation and material selection

3.1 Simulation software

The PC1D simulation method can simulate the photoelectric conversion effect of solar cells under sunlight, and obtain the simulation results of a series of important output parameters of solar

Т. 8. №6. 2022
https://doi.org/10.33619/2414-2948/79

cells, which can speed up the research progress of photovoltaic devices and provide important guidance for the development of new processes, as shown in Figure 3-1.

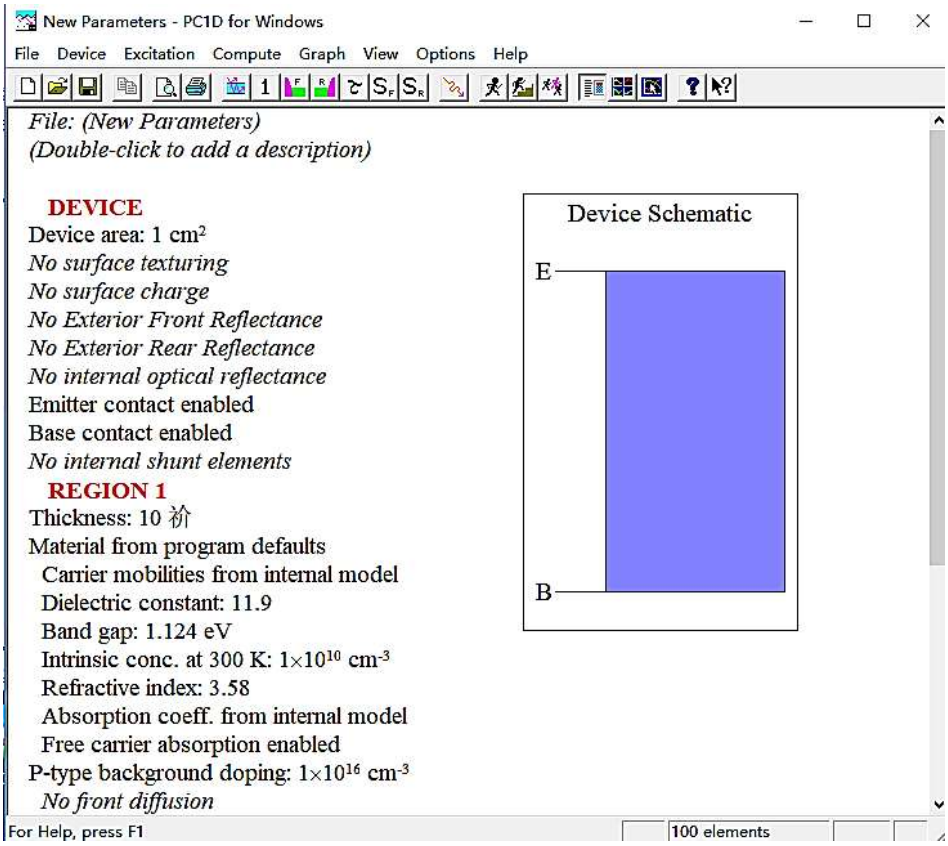

Figure 3-1. PC1D software simulation interface

3.2 physical equations of semiconductor devices and boundary conditions of solar cells

The relationship between electric field intensity E, charge density, electron and hole concentration n and P, electron hole current density Jn and Jp, generation rate and recombination rate G and U of electron hole pairs in semiconductor devices follows certain physical laws, which is reflected in multiple differential equations between these physical quantities. Its one-dimensional form is listed and briefly annotated as follows [13]:

$$\frac{dE}{dx} = \frac{\varphi}{\varepsilon} \tag{3-1}$$

$$Jn = q\mu_n(nE + \frac{k_0 T}{q}\frac{dn}{dx}) \tag{3-2}$$

$$Jp = q\mu_p(pE + \frac{k_0 T}{q}\frac{dp}{dx}) \tag{3-3}$$

$$\frac{1}{q}\frac{dJ_n}{dx} = U_n - G \tag{3-4}$$

$$\frac{1}{q}\frac{dJ_p}{dx} = G - U_p \tag{3-5}$$

Т. 8. №6. 2022
https://doi.org/10.33619/2414-2948/79

One dimensional simplification is suitable for the case that all physical quantities are uniform and unchanged in Y and Z directions. For solar cells, the thickness direction of the cell is taken as the X direction, and the plane direction of the cell is regarded as uniform. In many cases, it is a reasonable simplified approximation, which is suitable for calculating and analyzing many basic problems.

The charge density should include various contributions, so $q = PN + n - n_a$ .For solar cells, the generation rate G of electrons or holes should be related to the incident light intensity Q, the light absorption system a of the battery material and the depth x (x = 0 at the surface)

$$G = \alpha Q(1-R)\exp(-\alpha x) \tag{3-6}$$

We substitute them into the group of differential equations (Jp-5, including 3 pairs of unknown numbers, jn-5), and finally obtain the group of equations (Jp-3, jn-5). The (P,N,Jp,Jn,e) of solar cells with different one-dimensional structures obey this set of equations, which can be solved by this set of equations. The differences are fully reflected in their boundary conditions, material properties and cell structure. The results are completely different due to different conditions.

The boundary conditions include the composite velocity between the surface and the back, the electrical contact between the surface and the back, etc; The material properties include two kinds of carrier lifetime, two kinds of carrier mobility, absorption coefficient, dielectric constant and so on; The cell structure is all contained in the donor and acceptor doping concentration distribution, including abrupt p-n junction and transition gradual p-n junction, deep junction and shallow junction, and so on.

After the equations and the boundary conditions and structure of a specific solar cell are determined, the operation output of the solar cell under stable light can be solved theoretically. But generally, it can only be achieved by numerical calculation method and computer calculation. Such calculation is often called simulation. Pa. basore and others from the school of photovoltaic and renewable energy engineering of the University of New South Wales have released the calculation and simulation software PC1D for solving one-dimensional solar cell problems based on the difference method for free since the 1980s. Over the years, it has been widely used and recognized all over the world, and has been continuously revised and improved. The version has been updated more than 10 times (the current version is 5.9), It is a reliable, convenient and practical software for solar cell analysis and design optimization. We will further introduce its operation and application below.

3.3 PC1D operation

PC1D can calculate and analyze solar cells with different materials and different multilayer structures, and provide users with some materials and auxiliary lighting parameters or models, among which the characteristic data of crystalline silicon is the most complete[14].

After the program is started, the parameter interface is presented first. Click each parameter to open the parameter input window. There are no less than 40 parameters to be entered. Some parameters such as battery temperature and thickness are self-evident; However, the exact meaning of many parameters is difficult to determine at the moment, or its value is difficult to determine at the moment. To start the calculation, one cannot be vague. This is often very frustrating and daunting. A shortcut is suggested: click the file open button to call in the example of p-type solar cell parameter file provided to users in the software package, Pvcell, PRM. After the file is opened,

it will automatically load a full set of parameters or options of a typical p-type solar cell. Most of these parameters are basically fixed for crystalline silicon cells, and even the influence of temperature change has been taken into account in the input model. In this way, only the parameters that need to be determined and input are left for us to study. Next, we will introduce the important parameters one by one according to the order they appear on the parameter interface, but the meaning is not easy to understand or needs to be supplemented.

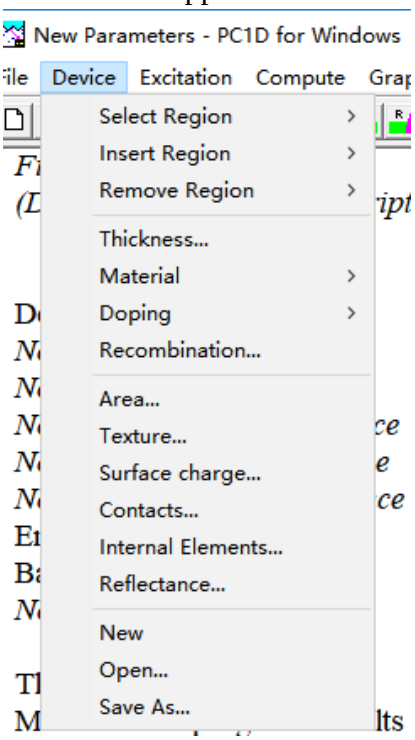

Figure 3-2. device drop-down submenu

3.3.1 Device parameters

(1) Surface charge surface external electrical contact condition option. Generally, ohmic contact shall be achieved for the battery, and neutral shall be selected. If there is a potential barrier on the surface, the accumulation of charge is a bad situation

(2) Emitter contact / base contact contact resistance. All series resistors are the sum of these two terms. Therefore, there is no need to stick to the parameter name, and the grid resistance should also be added here. For solar cells, the distance from the base contact to the surface can be any value greater than the thickness of the battery.

(3) Internal drain elements - internal drain element option. For silicon wafer batteries, basically only "internal conductor" needs to be considered, which is expressed in conductance, and its unit is Seimens (Siemens)

3.3.2 Material parameters

The program can deal with the partition of different materials (heterojunction). For silicon wafer battery, there is only one region. Front diffusion/rear diffusion-front

/back diffusion doping option. The program provides a double diffusion layer option. Generally, there is no need to set up a second layer. Interested readers can use it to study the double-layer effect, but there is no such practice in actual production and R &D.Bulk recombination/surface recombination-in vivo recombination/surface

recombination parameters. The program uses SRH model to calculate the recombination rate. The ET input in the upper part of the window is the recombination center (carrier trap) energy level.

Т. 8. №6. 2022
https://doi.org/10.33619/2414-2948/79

In the model, it is assumed that all the composite trap energy levels in the system are classified into one,which is expressed by the difference between it and the material intrinsic Fermi energy level (close to the midpoint of the band gap). Generally, input 0 represents the deepest trap; The lifetime Tau-n, Tau-p or recombination velocities S-N and S-P of the two kinds of carriers are "intrinsic", that is, the lifetime without donor or acceptor doping and nonequilibrium excitation. At this time, there is no distinction between majority carriers and minority carriers; The lower part of the window calculates the minority carrier lifetime or surface minority carrier recombination rate calculated under the set background doping type and concentration (substrate doping concentration) at 300K. The user can input the latter in the lower part of the window in turn, and the program will calculate and display the former in the upper part of the window.

3.3.3 excitation parameters

Irradiation conditions generally accept the standard AM1.5G irradiation parameters or options loaded in this example, i.e. exception mode and base circuit, which actually belong to some supporting options in the numerical simulation algorithm, and follow the recommended parameters loaded by the program author in this typical example. After the parameters are complete, click Run (the "single person run" button at the top right of the page) to get the calculation result instantly: the most important parameters in, V and P are immediately displayed at the bottom of the page; If you want to observe some parameters, such as carrier concentration distribution, I-V characteristics and even quantum efficiency, you can click the "four Diagrams" interface, in which the contents of each diagram can be selected by yourself; If you want to make an in-depth study of a certain figure, you can click the figure in the above interface to enter the "single figure" interface.

Finally, the most important function of PC1D, batch computing function, is introduced. Click the function button of the "three person run" logo to enter the batch parameter input window, and select a parameter to be investigated, its variation range, whether it is expressed in logarithm, and the number of average points. After that, click "OK" to return to the page, and then click "single person running" button, and all the calculation results will be listed in the lower part of the parameter interface page. Click "copy batch data" in the "graph" menu to paste them into the mapping software and draw them for analysis. The examples provided in this chapter are completed by batch processing method.

3.4 Selection of antireflection film materials for solar cells

In addition to its refractive index close to the target value when the antireflection effect is maximum, the ideal antireflection film material should have high transmittance and as small absorption coefficient as possible in the visible light area, and the stress of the film should be small. For multilayer antireflection films, the stress properties of adjacent layers should be opposite to avoid multilayer accumulation of stress. The films with compressive stress include ZnS, SiO_2, etc., and the films with tensile stress include Ta_2O_5, MgF_2, TiO_2 et al. [15], the film has good adhesion, stable physical and chemical properties, simple preparation process, environmental protection and low price.

The antireflection thin film materials studied more include MgF_2, TiO_2, SiO_2, Al_2O_3, etc. sin is mostly used as single-layer antireflection thin film materials in industry, mainly considering its passivation effect. The preparation process is plasma chemical vapor deposition, but the raw silane is easy to explode and dangerous. If the EVA package of solar cell is considered, the optimal refractive index of single-layer antireflection thin film is 2.45, while sin is only 1.9, The requirements for high and low refractive index layers of double-layer antireflection films are not suitable, and passivation can be realized by a certain process. Considering the optical properties, stability, preparation process and production cost of thin film materials, the ideal materials are TiO_2

Т. 8. №6. 2022
https://doi.org/10.33619/2414-2948/79

and SiO_2. TiO_2 can be used as high refractive index antireflection film materials and SiO_2 can be used as low refractive index antireflection film materials[18]. Both materials have their own unique advantages.

TiO_2 thin film is a material with high refractive index (2.2~2.7) and low absorption coefficient. It has excellent transmission characteristics in the visible light region, chemical stability and dielectric insulation, as well as the functions of self-cleaning, sterilization and disinfection. It is widely used in the optical and electronic fields [14-17]. At the same time, studies have shown that the optical properties of TiO2 thin films change with different process conditions, which can realize the adjustable change of refractive index of TiO2 thin films and achieve the best matching antireflection effect according to different needs. TiO_2 thin films used in solar cells can also promote the formation of TiSi alloy, so as to reduce the contact stiffness of the battery and further improve the efficiency of the battery. Therefore, TiO_2 is a promising antireflection film material for solar cells.

SiO_2 film is a material with high light transmittance and low extinction coefficient. The film has many advantages, such as strong hardness, good adhesion with the substrate, fine and dense structure, good wear resistance and so on. It is an important dielectric material,

Commonly used as passive film, protective film and insulating film of semiconductor devices. It has a wide application prospect in the fields of semiconductor and integrated circuit, optical components, optoelectronic devices and so on. SiO_2 film has low refractive index, which is the most suitable material for low refractive index layer of multilayer antireflection film.

SiO_2/TiO_2 double-layer film system is the most ideal solar cell antireflection film considering both antireflection effect and process cost. The film design is relatively perfect, and the coating process is mature and stable. After comprehensive consideration of various factors, TiO_2, MgF_2, Al_2O_3 and SiO_2 monolayer films were finally selected in this study; The properties of SiO_2/TiO_2, TiO_2/MgF_2, MgF_2/Al_2O_3 and SiO_2/Al_2O_3 bilayers were analyzed and compared.

4 PC1D Simulation Research

4.1 working principle of antireflection film

Solar cell antireflection film is an optical film deposited on the surface of solar cell or with multi-layer refractive index between incident medium and silicon substrate. It uses the reflected light formed by sunlight at each interface to reduce the reflectivity. According to the principle of optical interference, when the optical path difference of two beams is odd times of half wavelength, equation (4-1) is satisfied, and the interference of two beams will be eliminated.

$$\delta = (2k+1)\frac{\lambda}{2}, \quad k = 0,1,2,3..... \tag{4-1}$$

When the optical path difference of the two beams is an integral multiple of the wavelength, equation (4-2) is satisfied, and the two beams interfere and grow.

$$\delta = k\lambda, \quad k = 0,1,2,3..... \tag{4-2}$$

4.2 Initial value setting

The cell model used in this chapter is a standard buried grid solar cell structure. With solar spectrum AM1.5G is the light source, the energy density is 0.1w/cm^2, the working temperature is set to 25℃, the area size of solar cell is set to l00cm^2, and the reflectivity data of antireflection film is used as the input of PC1D software to calculate the short-circuit current, open circuit voltage and output power of solar cells with different antireflection films.

Т. 8. №6. 2022
https://doi.org/10.33619/2414-2948/79

4.3 research on single layer antireflection film

The structure of single-layer antireflection film is the simplest, and the structural diagram is shown in Figure 4-1.

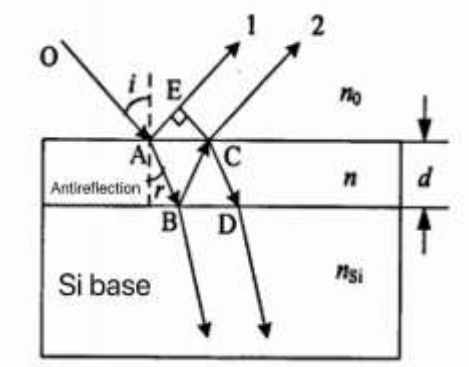

Figure 4-1. Structural diagram of single layer antireflection film

In the figure, the thickness of the film is D, the refractive index is n, the refractive index of the incident medium is N0, and the refractive index of the silicon substrate is n_{Si}, which satisfies $n_0 < n < n_{Si}$. When wavelength λ When the incident light OA irradiates the upper surface of the film at an angle I, the beam 1 will be formed after being reflected at point a. The refracted beam entering the film is ab, and R is the refraction angle. When the refracted beam AB reaches point B on the lower surface of the film, it will be reflected to form beam BC, and beam BC will finally refract from point C on the upper surface to form beam 2. Optical path difference between beam 1 and beam 2δ It can be expressed as:

$$\delta = n(AB + BC) - n_0 AE \tag{4-3}$$

Light from optically sparse medium to optically dense medium will produce half wave loss, and there is no half wave loss from optically dense medium to optically sparse medium. Because the light beam passes through the upper interface of the film from the light sparse medium to the light dense medium, the two reflected light will produce half wave loss, which is offset in the formula for calculating the optical path difference. As shown in Figure 4-1, each parameter has the following relationship:

$$\mathrm{AB} = \mathrm{BC} = \frac{d}{\cos r}, \quad AE = AC \cdot \sin i = 2d \cdot tgr \cdot \sin i \tag{4-4}$$

Combined with the refraction law: $n_0 \sin i = n \sin r$, it can be solved as follows:

$$\delta = n \cdot \frac{2d}{\cos r} - n_0 \cdot 2d \cdot tgr \cdot \sin i = n \cdot 2d \cdot (1 - \sin r) \cdot \frac{1}{\cos r} = 2nd \cos r \tag{4-5}$$

For a brief analysis, only the case of vertical incidence of light is discussed below. The optical path difference formula is simplified as： $\delta = 2nd$, when the optical thickness of the film is $nd = \frac{1}{4}\lambda$, $\delta = \frac{1}{2}\lambda$, beams 1 and 2 will interfere and cancel, and the reflected light will be weakened.

Similarly, it can be calculated that the optical path difference of transmitted beams 3 and 4 when light is incident vertically is:

Т. 8. №6. 2022
https://doi.org/10.33619/2414-2948/79

$$\delta = 2nd + \frac{\lambda}{2} \tag{4-6}$$

When the optical thickness of the film is $nd = \frac{1}{4}\lambda$, $\delta = \lambda$, the optical path difference of transmitted beams 3 and 4 just meets the condition of interference phase length, and the transmitted light is strengthened.

When light is incident vertically, the surface reflectance r of the battery coated with a single-layer antireflection film is

$$\mathrm{R} = \frac{\mathrm{R}_1^2 + \mathrm{R}_2^2 + 2R_1\mathrm{R}_2\cos\Delta}{1 + R_1^2 + R_2^2 + 2R_1R_2\cos\Delta} \tag{4-7}$$

Where: R_1 and R_2 are the reflectivity of light from incident medium to film and from film to silicon respectively. According to Fresnel formula:

$$\mathrm{R}_1 = \frac{n_0 - n}{n_0 + n}, \quad \mathrm{R}_2 = \frac{n - n_{Si}}{n + n_{Si}} \tag{4-8}$$

Δ is the phase angle caused by the film thickness, which is given by the following formula:

$$\Delta = \frac{4\pi nd}{\lambda} \tag{4-9}$$

If the optical thickness of the film is $nd = \frac{1}{4}\lambda$, the reflectivity formula (4-7) is transformed into:

$$\mathrm{R}_\lambda = \left|\frac{n^2 - n_0 \times n_{Si}}{n^2 + n_0 \times n_{Si}}\right|^2 \tag{4-10}$$

To make reflectance $\mathrm{R}_\lambda = 0$, the following requirements are required:

$$n = \sqrt{n_0 \times n_{Si}} \tag{4-11}$$

Therefore, the best single-layer antireflection film requires that the optical thickness of the film is one fourth of the target wavelength, and the refractive index is the square root of the product of the refractive index of the incident medium and the substrate.

When the light is incident obliquely at a certain angle, the nano light can be used to replace the refractive index. For any wavelength, incident angle and polarization plane, the general formula of reflectivity can be obtained by matrix method.

According to the previous analysis, the single-layer antireflection film can theoretically achieve zero reflection at a specific wavelength. When designing the solar cell antireflection film, it is necessary to select an appropriate wavelength. The peak value of the ground solar spectral power is 500~600nm and the peak value of the spectral response of silicon is 800~900nm. Considering these two factors, 600nm is selected as the reference value. When packaging is not considered, the

Т. 8. №6. 2022
https://doi.org/10.33619/2414-2948/79

best value of refractive index of single-layer antireflection film is $n=\sqrt{n_0 n_{Si}}=\sqrt{3.94}\approx 1.98$, if EVA packaging isconsidered, the best value of refractive index is $n=\sqrt{n_0 n_{Si}}=\sqrt{1.52\times 3.94}\approx 2.45$.

Taking MgF_2 (n=1.38), SiO_2 (n=1.46), Al_2O_3 (n=1.9) and TiO_2 (n=2.3) materials as examples, there is an optimal thickness value for different materials, corresponding to the minimum reflectivity. According to the data in the curve of reflectivity of single-layer films of different materials with wavelength in Figure 4-1, combined with the data in the light source file AM1.5G in PC1D software, the wavelength is generally 410nm~1180nm, as shown in Figure 4-3.

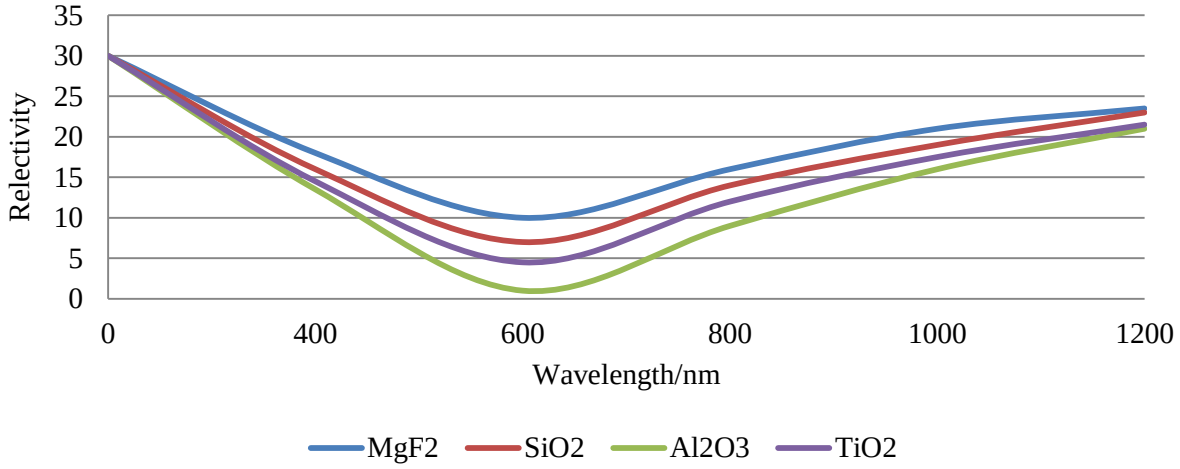

Figure 4-2. Single layer film reflectivity R with wavelength λ Change curve of

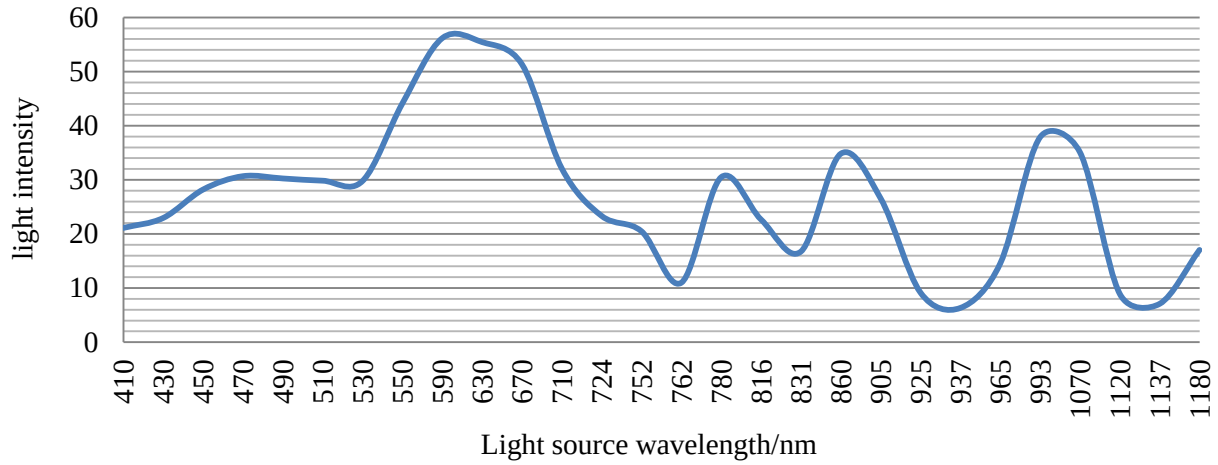

Figure 4-3. Light intensity corresponding to different wavelengths of light source

Combined with the data in the two figures, the transmission solar spectrum of the antireflection film is calculated with publicity (4-12)

$$Transmitted\ solar\ spectrum = (1-reflectance\ R)\times AM1.5\ solar\ intensity \quad (4\text{-}12)$$

Replace the second column of data in the AM1.5G file with the calculated result, rename the file to "AM1.5Gnew", select lighting-external file-Open AM1.5Gnew file in the excitation menu of PC1D, and then start data simulation with the antireflection film thickness of different materials. Fill the obtained battery output power into EXCEL, draw the curve between film thickness and battery output power, and get Figure 4-4, Figure 4-5, Figure 4-6 and Figure 4-7.

Т. 8. №6. 2022
https://doi.org/10.33619/2414-2948/79

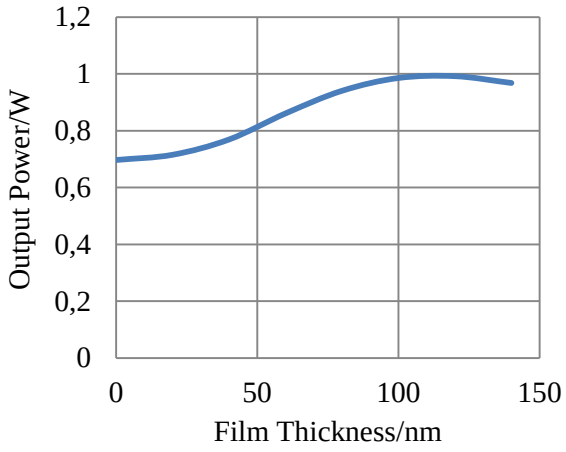

Figure4-4. Relationship between MgF2 single layer film thickness and battery output power

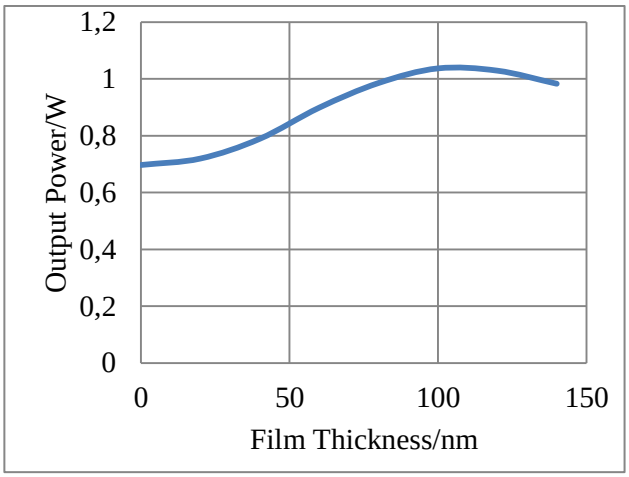

Figure 4-5. Relationship between SiO2 single layer film thickness and battery output power

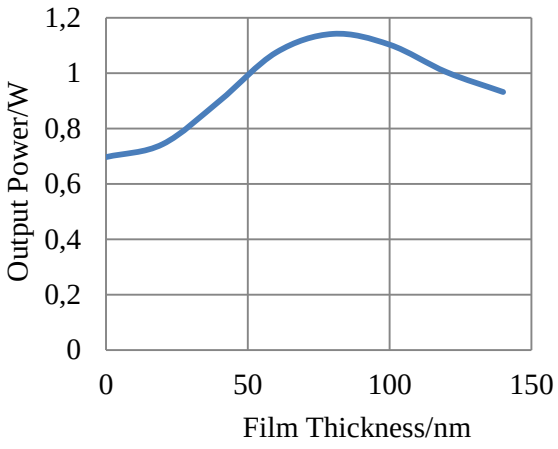

Figure 4-6. Relationship between Al_2O_3 single layer film thickness and battery output power

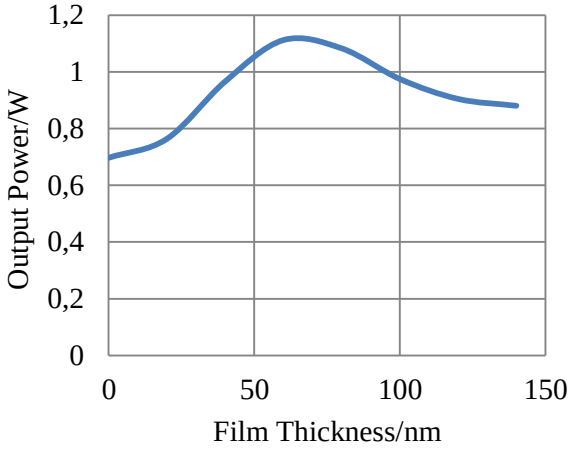

Figure 4-7. relationship between TiO_2 single layer film thickness and battery output power

Table 4-1 can be obtained from the above data.

Table 4-1

OPTIMUM THICKNESS AND OUTPUT POWER
OF SINGLE-LAYER FILM OF EACH MATERIAL

Single layer antireflection film material	*MgF_2*	*SiO_2*	*Al_2O_3*	*TiO_2*
Optimum thickness(nm)	105	94	72	60
Battery output power(W)	0.9908	1.025	1.131	1.112

4.4 Study on double-layer antireflection film

Single layer antireflection film can only achieve narrow-band antireflection, while multi-layer antireflection film can achieve low reflection in a wide wavelength range. Considering the preparation cost and optical properties, the double-layer antireflection film is an ideal choice for industrial production. The structure of double-layer antireflection film is shown in Figure 4-8.

Т. 8. №6. 2022
https://doi.org/10.33619/2414-2948/79

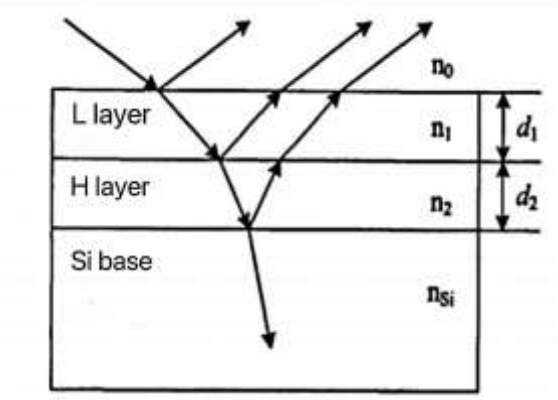

Figure 4-8. Structural diagram of double-layer antireflection film

In the figure, layer h is a high refractive index film, layer L is a low refractive index film, and the double-layer antireflection film usually adopts the gradient refractive index structure of $n_0<n_1<n_2<n_{Si}$ (incident medium, layer L, layer h and silicon substrate from top to bottom). When the optical thickness of the films is one quarter of the wavelength, that is $n_1d_1 = n_2d_2 = \frac{\lambda}{4}$, the surface reflectance r of the silicon cell coated with double-layer antireflection film can be expressed as:

$$R = \left(\frac{n_1^2 n_{Si} - n_2^2 n_0}{n_1^2 n_{Si} + n_2^2 n_0} \right)^2 \quad (4\text{-}12)$$

It can be seen from formula (4-12) that the reflectivity depends on the relationship between each refractive index. When $n_1^2 n_{Si} = n_2^2 n_0$, the wavelength λ The reflectivity at R= 0, the reflectivity curve of the film in the whole wavelength range is "V", which also belongs to narrow-band antireflection, but the low reflectivity range is wider than that of single-layer antireflection film. When $n_1 n_2 = n_{Si} n_0$, wavelength λ The reflectivity at is the maximum, but there are two minimum values with zero reflectivity on both sides of the wavelength. The reflectivity curve of the film is in the shape of "W", and lower reflectivity can be obtained in the whole solar spectrum (300-1200nm). Therefore, the optimum film thickness and refractive index of double-layer antireflection film are:

$$n_1 d_1 = n_2 d_2 = \frac{\lambda}{4} \quad (4\text{-}13)$$

$$n_1^3 = n_{Si} n_0^2, \quad n_2^3 = n_0 n_{Si}^2 \quad (4\text{-}14)$$

At the central wavelength of 600nm, the best refractive indexes of the double-layer antireflection film are:

$$n_1 = \sqrt[3]{n_0^2 n_{Si}} = \sqrt[3]{3.94} \approx 1.58, \quad n_2 = \sqrt[3]{n_0 n_{Si}^2} = \sqrt[3]{3.94^2} \approx 2.49$$

Take material a as an example. For different materials, there is an optimal thickness value corresponding to the minimum reflectivity. According to the data in the curve of reflectivity of bilayer films of different materials with wavelength in Figure 4-7, combined with the data in the light source file AM1.5G in PC1D software, the wavelength is generally 410nm-1180nm, as shown in Figure 4-3 above.

Combined with the data in the two figures, calculate the transmission solar spectrum of the antireflection film with publicity (4-12).

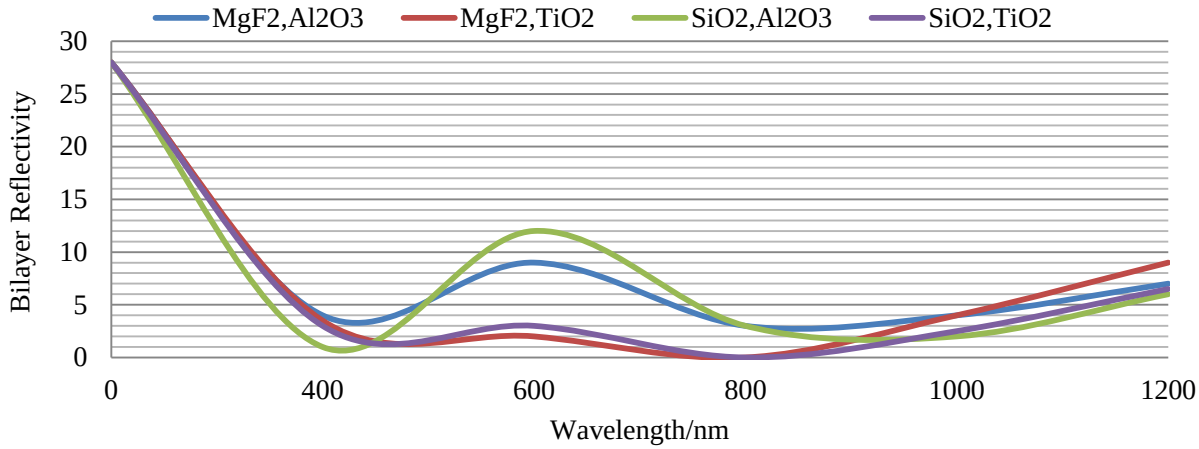

Figure 4-9. Reflectivity R of bilayer film with wavelength λ Change curve of

Taking SiO_2/TiO_2 as an example, first set the thickness of TiO_2 material as the fixed value and the thickness of SiO_2 material as the variable value, and simulates it with PC1D software, as shown in **Figure 4-10**

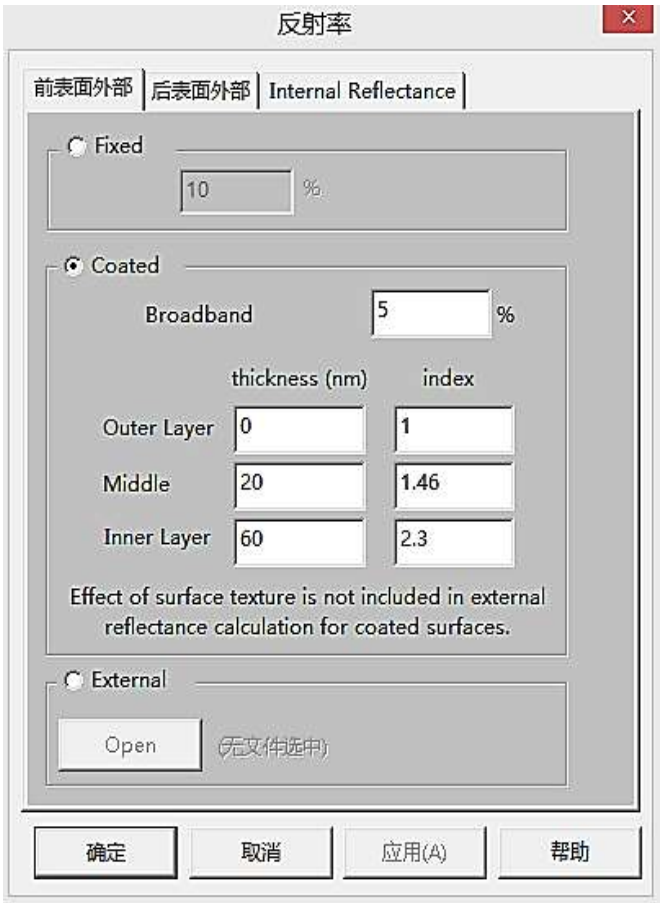

Figure 4-10. Simulation interface of double-layer film PC1D

It is the same as the above research data processing of single-layer antireflection film, and the curve is drawn with Excel.

Т. 8. №6. 2022
https://doi.org/10.33619/2414-2948/79

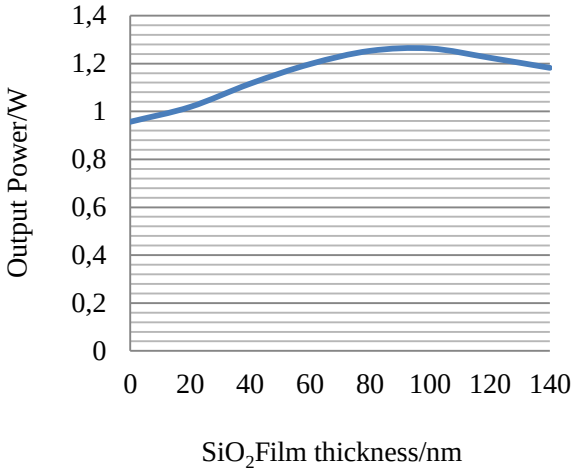

Figure 4-11. The Output power of the battery corresponding to the thickness of SiO2 film when the thickness of TiO_2 is a constant value of 20 nm

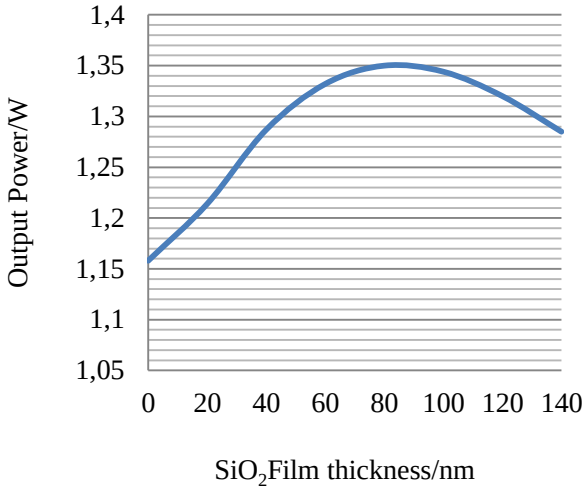

Figure 4-12. Battery output power corresponding to the thickness of SiO_2 film when the thickness of TiO_2 is a constant value of 40nm

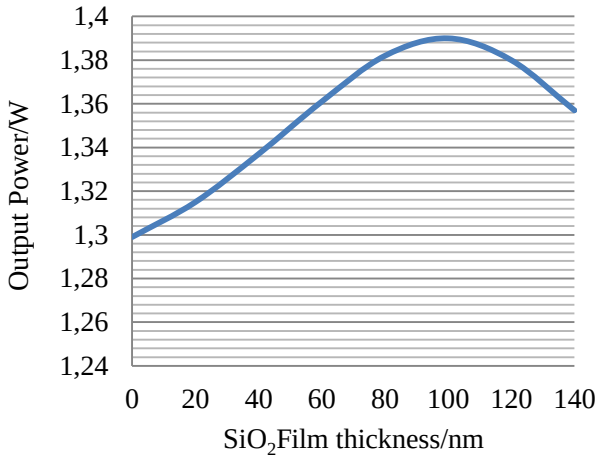

Figure 4-13. The output power of the battery corresponding to the thickness of SiO2 film when the thickness of TiO_2 is 60nm

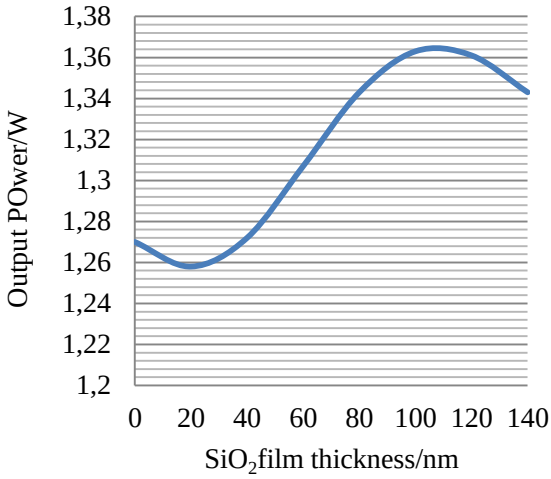

Figure 4-14. The output power of the battery corresponding to the thickness of SiO2 film when the thickness of TiO_2 is 80nm

It can be seen from the above data that when the thickness of TiO_2 material film is 60nm, the output power of the battery has a peak, so it can be concluded that when TiO_2 (d=60nm)/SiO_2 (d=94nm), the output power of the battery is the largest.

Using the same method, the optimal thickness of double-layer film of material TiO_2/MgF_2,MgF_2/Al_2O_3,SiO_2/Al_2O_3 is obtained by simulation, as shown in Table 4-2

Table 4-2

OPTIMUM THICKNESS AND BATTERY OUTPUT POWER OF DOUBLE-LAYER ANTIREFLECTION FILMS OF DIFFERENT MATERIALS

Double layer antireflection film material	*MgF_2/Al_2O_3*	*MgF_2/TiO_2*	*SiO_2/Al_2O_3*	*SiO_2/TiO_2*
Optimum thickness(nm)	100/72	100/60	94/72	94/60
Battery output power(W)	1.309	1.395	1.227	1.389

Т. 8. №6. 2022
https://doi.org/10.33619/2414-2948/79

4.5 design optimization of solar cell antireflection layer

4.5.1 change of film reflectivity before and after packaging

Generally speaking, batteries are used after packaging. After encapsulation, the incident medium adjacent to the antireflection film is silica gel between glass and the antireflection film (n=1.43), and then the reflectivity curve will change. Here, the changes of reflectivity curve of SiO_2/TiO_2 double-layer film system before and after battery packaging are given respectively (as shown in Figure 4-14). Obviously, the reflection curve of the encapsulated SiO_2/TiO_2 bilayer film is similar to that of the monolayer film. It has only very low reflectivity near the central wavelength point, which can not reduce the reflectivity in the whole wavelength range, so the anti reflection effect is not ideal. This is because the refractive index of the first film SiO_2 is equal to that of the incident medium silica gel, which degrades the bilayer film into an approximate monolayer film. Therefore, considering the packaging, the refractive index of the first layer of the double-layer film should be much greater than that of silica gel, and the refractive index of the second layer should also be increased, so as to have better antireflection effect. Combined with the existing antireflection film materials, I use MgO (n=1.74) and CeO_2 (n=2.4) as the top and bottom materials of the double-layer film respectively. The reflection curve of (MgO-14) / double-layer film is optimized, as shown in Figure 4-14. Obviously, compared with SiO_2/TiO_2 bilayer film, the optimized MgO (80 nm) /CeO_2 (60 nm) bilayer film has better reflection curve and better antireflection effect in the whole spectral response range of silicon.

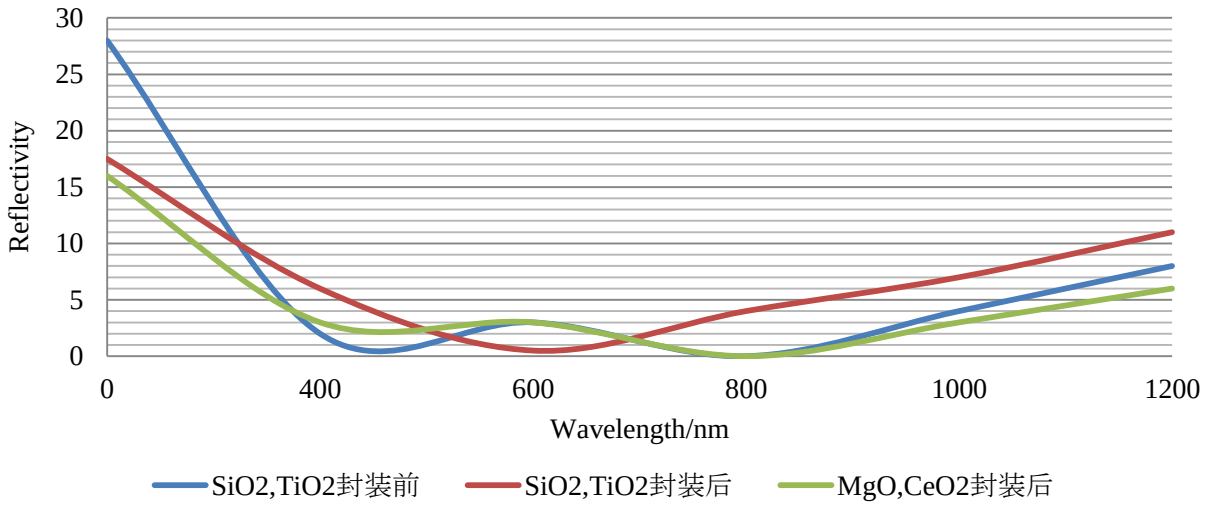

Figure 4-14. Reflectivity r of double-layer film before and after packaging with wavelength λ Change curve of

4.5.2 influence of passivation layer on antireflection film

The surface of most solar cells is passivated. There is a passivation layer with a thickness of 10~20nm between the cell substrate and the antireflection film, so the originally designed SiO_2/TiO_2 double-layer antireflection film is difficult to achieve the predetermined antireflection effect. In view of this phenomenon, the original antireflection film system is optimized. It is found that when the thickness of the second layer of TiO_2 is appropriately reduced, the anti reflection effect is improved. Table 4-3 shows the changes in the electrical properties of solar cells tested by Shanghai Aerospace Power Research Institute before and after coating and considering the optimization of passivation layer. As can be seen from Table 4-3, compared with that before

Т. 8. №6. 2022
https://doi.org/10.33619/2414-2948/79

coating, after coating antireflection films with two parameters respectively, the open circuit voltage is increased by 1.7%, the short-circuit current ISC is increased by 42.1% and 45.1% respectively, and the efficiency is improved η Increased by 45% and 47% respectively. Compared with the film system without passivation layer, the short-circuit current ISC of the battery is increased by 2.1% and the efficiency is improved η Increased by 1.4% [19].

Table 4-3

CHANGES OF BATTERY ELECTRICAL PERFORMANCE BEFORE AND AFTER ANTIREFLECTION FILM OPTIMIZATION WITH PASSIVATION LAYER

	Voc(mV)	*Isc(mA)*	*FF*	*η/%*
Before coating	600	235	0.782	10.2
After coating (before optimization)	610	334	0.782	14.8
After coating (after optimization)	610	341	0.782	15.0

According to the experimental results, we use the computer program to redesign the antireflection film of the battery with passivation layer in theory. We can redesign the double-layer antireflection film as a three-layer film (the passivation layer is the third layer of the film system), and adjust the original parameters of the double-layer film system. This is different from the general three-layer film design in that the parameters of the third layer film (refractive index n, thickness d) have been determined. In the design, according to the actual situation of the measured battery, the passivation layer is SiO_2(n=1.46, d=15nm), so the original SiO_2/TiO_2 double-layer film is changed into $SiO_2/TiO_2/SiO_2$(15nm) three-layer film. Curve a in Figure 4-15 is the reflectivity curve of SiO_2(94nm)/TiO_2(60nm) bilayer film applied to the battery without passivation layer. For the battery with passivation layer, the SiO_2(94nm)/ TiO_2(60nm) double-layer film actually becomes SiO_2(94nm)/TiO_2(60nm)/SiO_2 (15nm) three-layer film. At this time, the reflectivity curve is curve B.Obviously,the antireflection effect is not ideal So we changed the parameters of the original SiO2 / TiO_2 bilayer film to obtain the SiO_2(94nm)/TiO_2(40nm)/SiO_2(15nm) three-layer film curve C. It can be seen from curves B and C that when the thickness of the second film TiO_2 is reduced from 60nm to 40nm, the reflectivity decreases. This is consistent with the experimental result that appropriately reducing the thickness of the second film will improve the antireflection effect.

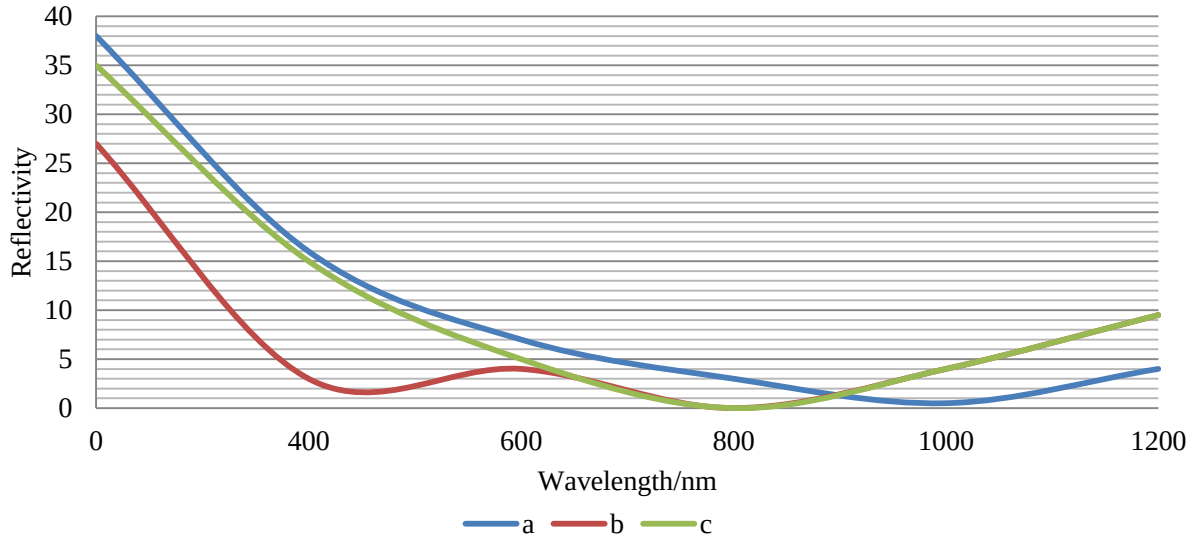

Figure 4-15. Effect of passivation layer on reflection curve

Т. 8. №6. 2022
https://doi.org/10.33619/2414-2948/79

5 Summary and Prospect

In this paper, the microstructure characteristics of the antireflection layer on the surface of crystalline silicon solar cell and its influence on the performance of the cell are studied in detail, and the influence of antireflection layer films of different materials on the cell is simulated by software. On this basis, the design of optimizing the antireflection layer on the surface of solar cell is proposed. Finally, the high-efficiency optimization parameters of the antireflection layer of crystalline silicon solar cell are obtained in the simulation of PC1D software. The main work includes the following aspects:

1. Study the optical design of solar cells. In addition to the photovoltaic effect of the basic solar cell, there are antireflection layer and suede, which also affect the output power of the cell.

2. Study on the influence of different materials of double-layer and reverse layer on the output of solar cells. The best thickness of antireflection layer of different materials is simulated and analyzed by PC1D software combined with the data in the light source file.

3. The antireflection film of solar cell is optimized by computer simulation. The optimal system parameters of antireflection film are obtained according to the reflectivity curve, and the influence of packaging and passivation layer on antireflection film is solved. Considering the packaging, the optimized MgO(80 nm)/CeO_2(60 nm)double-layer antireflection film has better antireflection effect. When there is passivation layer, the SiO_2/TiO_2 double-layer antireflection film is regarded as SiO2/TiO_2/SiO_2(15nm) three-layer antireflection film, and the optimization design is carried out.

In short, this paper studies and analyzes the antireflection layer on the surface of crystalline silicon solar cells, and puts forward the optimization method and carries out simulation, which lays a foundation for reducing the production cost of crystalline silicon cells.

References:

1. Wei, Guangpu (2006). Solar energy and sunshine economy. *Shanghai electric power,* (4): 338.

2. Lei, Yongquan (2000). New energy materials. Tianjin: Tianjin University Press.

3. Miles, R. W., Hynes, K. M., & Forbes, I. (2005). Photovoltaic solar cells: An overview of state-of-the-art cell development and environmental issues. *Progress in crystal growth and characterization of materials*, *51*(1-3), 1-42. https://doi.org/10.1016/j.pcrysgrow.2005.10.002

4. Zemin, J. (2008). Reflections on energy issues in China. *China Nuclear Power*, *1*.

5. Zhang, Shi, Wang, Xiaoping, Wang, Lijun (2010). Research progress of thin film solar cells. *Materials Guide: review, 24*(5), 126.

6. Chapin, D. M., Fuller, C. S., & Pearson, G. L. (1991). A new silicon pn junction photocell for converting solar radiation into electrical power. In *Semiconductor Devices: Pioneering Papers* (pp. 969-970). https://doi.org/10.1142/9789814503464_0138

7. Smits, F. M. (1976). History of silicon solar cells. *IEEE Transactions on Electron Devices*, *23*(7), 640-643. https://doi.org/10.1109/T-ED.1976.18465

8. Liu, Zuming, Li, jiehui, & Liao, Hua (2004). New progress in manufacturing technology of crystalline silicon solar cells [R] Proceedings of the 8th Photovoltaic Conference. P. 802-805.

9. Dong, Yufeng, Wang, Wanlu, & Han, Daxing (1999). American photovoltaic power generation and million roof plan, solar energy, (1): 29

10. Geng, Xinhua, Sun, Yun, & Wang, Zongpan (1999). Research progress of thin film solar cells. *Physics, 28*, 96.

Т. 8. №6. 2022
https://doi.org/10.33619/2414-2948/79

11. An, Qilin (2009). Principle and technology of solar cell. Shanghai: Shanghai Science and Technology Press.

12. Martin, Written (2010). Working principle, technology and system application of solar cell. Shanghai: Shanghai Jiaotong University Press.

13. Yan, Hui (2004). Research on high-precision plating with high reflection. Helie: Hefei University of technology.

14. Straumal, B. B., Vershinin, N. F., Cantarero-Saez, A., Friesel, M., Zieba, P., & Gust, W. (2001). Vacuum arc deposition of protective layers on glass and polymer substrates. *Thin Solid Films*, *383*(1-2), 224-226. https://doi.org/10.1016/S0040-6090(00)01799-5

15. Zheng, S. K., Wang, T. M., Xiang, G., & Wang, C. (2001). Photocatalytic activity of nanostructured TiO2 thin films prepared by dc magnetron sputtering method. *Vacuum*, *62*(4), 361-366. https://doi.org/10.1016/S0042-207X(01)00353-0

16. Hovel, H. J. (1978). TiO2 antireflection coatings by a low temperature spray process. *Journal of the Electrochemical Society*, *125*(6), 983.

17. DeLoach, J. D., Scarel, G., & Aita, C. R. (1999). Correlation between titania film structure and near ultraviolet optical absorption. *Journal of applied physics*, *85*(4), 2377-2384. https://doi.org/10.1063/1.369553

18. Kamataki, O., Iida, S., Saitoh, T., & Uematsu, T. (1990, May). Characterization of antireflection films for surface-passivated crystalline silicon solar cells using spectroscopic ellipsometry. In *IEEE Conference on Photovoltaic Specialists* (pp. 363-367). IEEE. https://doi.org/10.1109/PVSC.1990.111649

Список литературы:

1. Guangpu Wei. Solar energy and sunshine economy // Shanghai electric power. 2006. №4. P. 338.

2. Lei Yongquan. New energy materials. Tianjin: Tianjin University Press, 2000.

3. Miles R. W., Hynes K. M., Forbes I. Photovoltaic solar cells: An overview of state-of-the-art cell development and environmental issues // Progress in crystal growth and characterization of materials. 2005. V. 51. №1-3. P. 1-42. https://doi.org/10.1016/j.pcrysgrow.2005.10.002

4. Zemin J. Reflections on energy issues in China // China Nuclear Power. 2008. V. 1.

5. Zhang Shi, Wang Xiaoping, Wang Lijun, et al. Research progress of thin film solar cells // Materials Guide: review. 2010. V. 24. №5. P. 126

6. Chapin D. M., Fuller C. S., Pearson G. L. A new silicon pn junction photocell for converting solar radiation into electrical power // Semiconductor Devices: Pioneering Papers. 1991. P. 969-970. https://doi.org/10.1142/9789814503464_0138

7. Smits F. M. History of silicon solar cells // IEEE Transactions on Electron Devices. 1976. V. 23. №7. P. 640-643. https://doi.org/10.1109/T-ED.1976.18465

8. Liu Zuming, Li jiehui, Liao Hua, et al. New progress in manufacturing technology of crystalline silicon solar cells // Proceedings of the 8th Photovoltaic Conference. 2004. P. 802-805

9. Dong Yufeng, Wang Wanlu, Han Daxing, American photovoltaic power generation and million roof plan, solar energy. 1999. №1. P. 29.

10. Geng Xinhua, Sun Yun, Wang zongpan, etc Research progress of thin film solar cells Physics. 1999. №28. P. 96.

11. An Qilin et al Principle and technology of solar cell. Shanghai: Shanghai Science and Technology Press, 2009.

12. Martin Written by green, translated by Di David, Cao Zhaoyang, Li Xiuwen, etc Working principle, technology and system application of solar cell. Shanghai: Shanghai Jiaotong University Press, 2010.

13. Yan Hui Research on high-precision plating with high reflection. Helie: Hefei University of technology, 2004.

14. Straumal B. B. Vacuum arc deposition of protective layers on glass and polymer substrates // Thin Solid Films. 2001. V. 383. №1-2. P. 224-226. https://doi.org/10.1016/S0040-6090(00)01799-5

15. Zheng S. K., Wang T. M., Xiang G., Wang C. Photocatalytic activity of nanostructured TiO2 thin films prepared by dc magnetron sputtering method // Vacuum. 2001. V. 62. №4. P. 361-366. https://doi.org/10.1016/S0042-207X(01)00353-0

16. Hovel H. J. TiO2 antireflection coatings by a low temperature spray process // Journal of the Electrochemical Society. 1978. V. 125. №6. P. 983.

17. DeLoach J. D., Scarel G., Aita C. R. Correlation between titania film structure and near ultraviolet optical absorption // Journal of applied physics. 1999. V. 85. №4. P. 2377-2384. https://doi.org/10.1063/1.369553

18. Kamataki O., Iida S., Saitoh T., Uematsu T. Characterization of antireflection films for surface-passivated crystalline silicon solar cells using spectroscopic ellipsometry // IEEE Conference on Photovoltaic Specialists. IEEE, 1990. P. 363-367. https://doi.org/10.1109/PVSC.1990.111649

Работа поступила
в редакцию 04.05.2022 г.

Принята к публикации
11.05.2022 г.

Ссылка для цитирования:

Yilie Zhao Design and Analysis of Antireflection Layer on the Surface of Crystalline Silicon Solar cell // Бюллетень науки и практики. 2022. Т. 8. №6. С. 470-491. https://doi.org/10.33619/2414-2948/79/48

Cite as (APA):

Yilie, Zhao (2022). Design and Analysis of Antireflection Layer on the Surface of Crystalline Silicon Solar cell. *Bulletin of Science and Practice, 8*(6), 470-491. https://doi.org/10.33619/2414-2948/79/48